

1 Impact of age-specific immunity on the timing and burden of 2 the next Zika virus outbreak

3 Michel J. Counotte^{1,2}, Christian L. Althaus¹, Nicola Low¹, and Julien Riou¹

4 ¹Institute of Social and Preventive Medicine, University of Bern, Bern, Switzerland

5 ²Graduate School for Cellular and Biomedical Sciences, University of Bern, Bern,
6 Switzerland

7 July 10, 2019

8 **Abstract**

9 The 2015–2017 epidemics of Zika virus (ZIKV) in the Americas caused widespread protective
10 immunity. The timing and burden of the next Zika virus outbreak remains unclear. We used an
11 agent-based model to simulate the dynamics of age-specific immunity to ZIKV, and predict the
12 future age-specific risk using data from Managua, Nicaragua. We also investigated the potential
13 impact of a ZIKV vaccine. Assuming lifelong immunity, the risk of a ZIKV outbreak will remain
14 low until 2035 and rise above 50% in 2047. The imbalance in age-specific immunity implies that
15 people in the 15–29 age range will be at highest risk of infection during the next ZIKV outbreak,
16 increasing the expected number of congenital abnormalities. ZIKV vaccine development and
17 licensure are urgent to attain the maximum benefit in reducing the population-level risk of
18 infection and the risk of adverse congenital outcomes. This urgency increases if immunity is not
19 lifelong.

20 **1 Introduction**

21 Zika virus (ZIKV) is a flavivirus, which is transmitted primarily by mosquitoes of the genus *Aedes*.
22 Before 2007, circulation of the virus only occurred sporadically in African and Asian countries
23 (Wikan and Smith, 2016; Kohl and Gatherer, 2015). Between 2007 and 2013, ZIKV caused large-
24 scale epidemics in the populations of Micronesia (Duffy et al., 2009), French Polynesia (Cao-Lormeau
25 et al., 2014) and other Pacific islands (Wikan and Smith, 2016). ZIKV probably became established
26 in *Aedes aegypti* mosquitoes in the Americas between 2013-2014, (Faria et al., 2016; Zhang et al.,
27 2017) and then spread rapidly across the continent. In 2015, doctors in Brazil started reporting
28 clusters of infants born with microcephaly, a severe congenital abnormality, and of adults with
29 Guillain-Barré syndrome, a paralyzing neurological condition, resulting in the declaration by the
30 World Health Organization (WHO) of a Public Health Emergency of International Concern (PHEIC)
31 (World Health Organization, 2016). WHO stated, in September 2016, that ZIKV in pregnancy was
32 the most likely cause of the clusters of microcephaly, and other adverse congenital outcomes (Krauer
33 et al., 2017; Counotte et al., 2018). The risk of an affected pregnancy appears highest during the first
34 trimester, with estimates between 1.0 and 4.5% (Cauchemez et al., 2016; Johansson et al., 2016).
35 By the beginning of 2018, over 220,000 confirmed cases of ZIKV infection had been reported from
36 Latin America and the Caribbean (PAHO, 2019), which is estimated to be only 1.02% (\pm 0.93%) of
37 the total number of cases, based on mathematical modelling studies (Zhang et al., 2017).

38 Protective immunity conferred by infection, combined with high attack rates and herd immunity,
39 can explain the ending of epidemics and the lack of early recurrence (Dietz, 1975), as has been seen

40 with ZIKV (Ferguson et al., 2016). The duration of protective immunity induced by ZIKV infection
41 remains uncertain, since immunity to ZIKV infection was not studied extensively before the 2013
42 outbreaks. Evidence from seroprevalence studies in French Polynesia and Fiji found that levels of
43 ZIKV neutralizing antibodies decrease with time (Henderson et al., 2019). If the fall in antibody
44 levels means that people become susceptible to infection again, population level ZIKV immunity
45 might be declining already. Even if protective immunity is lifelong, the risk of a new ZIKV outbreak
46 will rise as susceptible newborns replace older individuals, lowering the overall proportion of the
47 population that is immune. A modelling study, based on data from the 2013 epidemic in French
48 Polynesia, estimated that ZIKV outbreaks are unlikely to occur for 12 to 20 years, assuming lifelong
49 immunity (Kucharski et al., 2016).

50 A direct consequence of population renewal will be an unequal distribution of immunity by age
51 group, with younger age groups at higher risk from a new epidemic than older people (Ferguson
52 et al., 2016). That effect will be amplified if ZIKV attack rates are lower in children than adults.
53 Assessing the risk of ZIKV infection in women of reproductive age is essential because ZIKV infection
54 in pregnancy, leading to adverse congenital outcomes, has such important implications for individ-
55 uals, for public health and for investment in surveillance and mitigation strategies, including vector
56 control, early warning systems, and vaccines (Abbink et al., 2018; World Health Organization, 2018).
57 However, currently no vaccine is available against ZIKV. Phase I clinical trials of ZIKV candidate
58 vaccines have shown levels of neutralizing antibody titers that were considered protective against
59 reinfection (Gaudinski et al., 2018; Modjarrad et al., 2018). Some vaccines have already entered
60 phase II trials (National Institute of Allergy and Infectious Diseases, 2018), but some companies
61 have stopped vaccine development (Cohen, 2018).

62 Researchers in Managua, Nicaragua were the first to report the age-stratified seroprevalence
63 of ZIKV antibodies in population-based surveys (Zambrana et al., 2018). The first cases of au-
64 tochthonous ZIKV infection in Nicaragua were reported in January, 2016, and an epidemic was
65 observed between July and December of that year. Through case-based surveillance, the public
66 health authorities of Nicaragua reported a total of 2,795 people with ZIKV detected by reverse tran-
67 scriptase (RT) PCR over this period (PAHO, 2019). The number of symptomatic infections is likely
68 much higher, owing to under-reporting. Furthermore, ZIKV infection is asymptomatic in 33 to 87%
69 of cases [23], which are generally not identified by surveillance systems. Shortly after the end of the
70 2016 epidemic, Zambrana et al. analyzed sera from two large population-based surveys in Managua
71 to measure the prevalence of IgG antibodies against ZIKV in 2- to 14-year olds ($N=3,740$) and 15-
72 to 80-year olds ($N=2,147$) (Zambrana et al., 2018). The authors reported ZIKV seroprevalence of
73 36.1% (95% confidence interval, CI: 34.5; 37.8%) among the 2-14 year age group and 56.4% (95% CI:
74 53.1; 59.6%) among the 15-80 year age group (Zambrana et al., 2018; Balmaseda et al., 2017). The
75 observed post-outbreak seroprevalence in adults is in line with findings from seroprevalence studies
76 from French Polynesia, Brazil, and Bolivia (Aubry et al., 2017; Netto et al., 2017; Saba Villarroel
77 et al., 2018).

78 In this study, we used data from the 2016 ZIKV epidemic in Managua and developed an agent-
79 based model (ABM) to predict the evolution of age-specific protective immunity to ZIKV infection
80 in the population of Managua, Nicaragua during the period 2017–2097. We assessed: 1) the risk of
81 a future ZIKV outbreak; 2) the consequences of a future ZIKV outbreak on women of reproductive
82 age; 3) the influence of loss of immunity on future attack rates; and 4) how vaccination could prevent
83 future ZIKV outbreaks.

84 2 Methods

85 2.1 Modelling strategy

86 We assessed the consequences of future outbreaks of ZIKV infection in Managua, Nicaragua using
87 a stochastic ABM. The model follows a basic susceptible-infected-recovered (SIR) framework and

Table 1: Parametrization of the agent-based model. ^aage-dependent parameters; ^bthe different scenarios are discussed in the text in detail under the headings corresponding to the headings of this table.

Parameter	Comment	Source
ZIKV epidemic parameters		
Transmission rate ^a	Inferred from the 2016 epidemic	Zambrana et al. (2018)
Recovery rate	Inferred from the 2016 epidemic	Zambrana et al. (2018)
ZIKV immunity		
Initial immunity ^a	Inferred from the 2016 epidemic	Zambrana et al. (2018)
Duration of immunity	Lifelong or decaying with time	5 scenarios ^b
Demography		
Initial age distribution	–	World Bank (2019a)
Birth rate	–	World Bank (2019a)
Death rate ^a	–	World Health Organization (2019)
Ageing	Linear ageing at each time-step	–
ZIKV reintroduction		
Delay until reintroduction	1 to 80 years	80 scenarios ^b
Cases reintroduced	1, 5 or 10 cases	3 scenarios ^b
Risk of adverse congenital event		
Exposure	Proportion of women in the first semester of pregnancy	World Bank (2019a)
Risk of microcephaly	Upon infection during exposure time (3 levels of risk)	Cauchemez et al. (2016); Johansson et al. (2016)
Targeted vaccination		
Date of implementation	In 2021, 2025 or 2031	3 scenarios ^b
Effective coverage	Proportion of 15 year old girls vaccinated (0% to 80%)	5 scenarios ^b

88 integrates processes related to ZIKV transmission, immunity, demography, adverse congenital out-
 89 comes and vaccination (Table 1). We parameterized the model based on published estimates or
 90 inferences from data about the 2016 ZIKV epidemic (Table 1). We considered different scenarios
 91 about the duration of immunity, the timing and scale of ZIKV reintroductions in the population,
 92 and the timing and scale of a hypothetical vaccination program targeted towards 15 year old girls.

93 2.2 Model structure

94 We simulated a population of 10,000 individuals for 80 years (2017–2097). We assigned agents age
 95 and ZIKV infection status (susceptible S , infected I or immune R). Initial conditions reflected the
 96 situation in Managua, Nicaragua in 2017, when there was no documentation of active transmission.
 97 In the outbreak-free period, we only considered demographic and immunity processes: births, deaths,
 98 ageing and, if applicable, loss of immunity and vaccination. Given the scarcity of these events
 99 at the individual level, we select a long time-step of seven days and stochastically applied the
 100 transition probabilities at each time step for each agent. After a given time, ZIKV-infected cases
 101 were reintroduced in the population. Upon reintroduction, the time step was reduced to 0.1 days, and
 102 we evaluated the epidemic-related transition probabilities: Susceptible agents may become infected
 103 at a rate $\beta_a I/N$, where β_a is the age-dependent transmission rate and N the total population size.
 104 Infected individuals may recover with a rate γ . We ignored the influence of the vector population

105 and assumed that the force of infection is directly proportional to the overall proportion of infected
106 individuals. We allowed six months for the outbreak to finish after introduction. Simulations
107 were conducted independently for each combination of scenarios and repeated 1,000 times. In the
108 baseline scenario, we assumed no vaccination, no loss of immunity and a reintroduction of 10 infected
109 individuals.

110 We implemented the model in ‘Stan’ version 2.18 (Carpenter et al., 2017) and we conducted
111 analyses with R version 3.5.1 (R Core Team and Team, 2008). The Bayesian inference framework
112 Stan permits the use of probability distributions over parameters instead of single values, allowing
113 for the direct propagation of uncertainty. Stan models are compiled in C++, which improves the
114 efficiency of simulations. Algorithm 1 (Appendix A.1) describes the ABM in pseudo code. The
115 model code and data are available from <http://github.com/ZikaProject/SeroProject>.

116 2.3 Parametrization

117 2.3.1 ZIKV epidemic parameters

118 We inferred the probability distributions for the age-specific transmission rate β_a and the recovery
119 rate γ from data on the 2016 ZIKV epidemic in Managua, Nicaragua. We used surveillance data
120 (Zambrana et al., 2018), which give weekly numbers of incident ZIKV infections, confirmed by
121 RT-PCR (dataset A, $n=1,165$), and survey data on age-stratified ZIKV seroprevalence, measured
122 among participants of pediatric and household cohort studies in Managua during weeks 5–32 of 2017
123 (dataset B, $n=3,740$ children and 1,074 adults) (Zambrana et al., 2018).

124 We conducted statistical inference using a deterministic, ordinary differential equation (ODE)-
125 based version of the ABM with three compartments (S , I and R) and two age classes ($a \in \{1, 2\}$)
126 corresponding to ages 0–14 and ≥ 15):

$$127 \frac{dS_a}{dt} = -\beta_a S_a \frac{\sum I_a}{N} \quad (1)$$

$$128 \frac{dI_a}{dt} = \beta_a S_a \frac{\sum I_a}{N} - \gamma I_a \quad (2)$$

$$129 \frac{dR_a}{dt} = \gamma I_a \quad (3)$$

131 We ignored demography in this model because it covers a short time span. We recorded the overall
132 cumulative incidence of ZIKV cases using a dummy compartment:

$$133 \frac{dC}{dt} = \sum_a \beta_a S_a \frac{\sum I_a}{N} \quad (4)$$

134 in order to compute the weekly incidence on week t :

$$135 D_t = C(t) - C(t - 1) \quad (5)$$

136 We fitted the model to weekly incidence data A using a normal likelihood after a square-root
137 variance-stabilizing transformation (Guan, 2009):

$$138 \Pr(\mathbb{A}|\beta_a, \gamma, \rho, \sigma) = \prod_t \mathcal{N}(\sqrt{\mathbb{A}}|\sqrt{\rho D}, \sigma) \quad (6)$$

139 where ρ is a reporting rate parameter and σ an error parameter. In addition, we also fitted the
140 model to the number of individuals with anti-ZIKV antibodies at the end of the epidemic by age
141 group \mathbb{B}_a using a binomial likelihood:

$$142 \Pr(\mathbb{B}|\beta_a, \gamma) = \prod_a \mathcal{B}(\mathbb{B}_a|n_a, p_a) \quad (7)$$

143 where B_a the number of individuals with antibodies, n_a is the sample size in each age group, and
 144 $p_a = R_a(t_{end})/N_a(t_{end})$ the proportion of immune at the end of the epidemic. The full likelihood
 145 was obtained by multiplying Eq. 6 and Eq. 7. We chose weakly-informative priors for all parameters
 146 and fitted the model in Stan (Table 2). We describe the calculation of the basic reproduction number
 147 \mathcal{R}_0 in appendix A.2. We used one thousand posterior samples for β_a and γ obtained by Hamiltonian
 148 Monte Carlo in the ABM model, ensuring the full propagation of uncertainty. Parameter values can
 149 translate from deterministic to agent-based versions of an epidemic model if the time step is small
 150 (Roche et al., 2011a), which was the reason for using a time step of 0.1 days.

Table 2: Parameter estimates inferred from incidence and sero-prevalence data on the 2016 ZIKV epidemic in Managua, Nicaragua. CrI: Credible interval.

Parameter	Interpretation	Prior	Posterior (median and 95% CrI)
β_1	Transmission for age group 0-14	Expon(0.1)	0.19 (0.16; 0.22)
β_2	Transmission for age group ≥ 15	Expon(0.1)	0.32 (0.30; 0.36)
$1/\gamma$	Duration of infectious period	Gamma(1, 0.1)	4.8 (4.3; 5.4)
ρ	Reporting rate	Beta(1, 1)	0.24% (0.21; 0.26)
$I(0)$	Initial number of infectious	Expon(0.1)	74 (40; 134)
\mathcal{R}_0	Basic reproduction number	–	1.58 (1.56; 1.59)

151 2.3.2 ZIKV immunity

152 We used the deterministic model, described in the previous section, to infer the proportion of people
 153 with protective immunity within each age group at the end of the 2016 epidemic \tilde{p}_a . We used one
 154 thousand posterior samples of \tilde{p}_a in the ABM to allow the propagation of uncertainty. Protective
 155 immunity to ZIKV after infection was lifelong in our first scenario, so the reduction of the overall
 156 proportion of immune individuals in the population decreased only because of population renewal.
 157 Given the absence of evidence about the duration of immunity to ZIKV, we considered four scenarios
 158 assuming exponentially distributed durations of immunity with means of 30, 60, 90, or 150 years.
 159 These values correspond to a proportion of initially immune agents that loses immunity after 10
 160 years of 28%, 15%, 11% or 6%, respectively (Appendix A.3).

161 2.3.3 Demography

162 We based the initial age distribution of the population on data from the World Bank (World Bank,
 163 2019b). We used age-dependent death rates for 2016 from the World Health Organization (World
 164 Health Organization, 2019). For births, we computed a rate based on an average birth rate in
 165 Nicaragua of 2.2 births per woman, which was uniformly distributed over the female reproductive
 166 lifespan (World Bank, 2019a). We defined the period of reproductive age between 15 and 49 years.
 167 The ageing process was linear, increasing the age of each agent by 7 days at each 7-day time step.

168 2.3.4 ZIKV reintroduction

169 We reintroduced ZIKV in the population after a delay of $d = \{1, \dots, 80\}$ years in independent
 170 simulations. We chose this approach rather than continuous reintroductions to remove some of
 171 the stochasticity and assess more clearly the association between immunity decay and risk of an
 172 outbreak. As the probability of an extinction of the outbreak depends on the number of ZIKV cases
 173 reintroduced in the population, we considered three different values for the seed (1, 5 or 10 cases)
 174 and compared the results (Appendix A.4). Simulations using continuous reintroductions each year
 175 are presented in the appendix A.5.

176 **2.3.5 Risk of adverse congenital outcomes**

177 The estimated number of microcephaly cases resulting from the reintroduction of ZIKV depended
178 on the exposure, i.e. the number of pregnant women infected by ZIKV during their first trimester,
179 to which we applied three different levels of risk, based on published estimates (Cauchemez et al.,
180 2016; Johansson et al., 2016). We obtained the number of ZIKV infections among women aged
181 15–49 years from ABM simulations. As gender was not explicitly considered in the model, we
182 assumed that women represented 50% of the population. We assumed a uniform distribution of
183 births during the reproductive period, and considered that the first trimester constituted a third
184 of ongoing pregnancies at a given time. We explored three different levels of risk of microcephaly
185 in births to pregnant woman with ZIKV infection during the first trimester, as reported by Zhang
186 et al., based on data from French Polynesia (0.95%, called low risk) and Brazil (2.19% and 4.52%,
187 called intermediate and high risk, respectively) (Cauchemez et al., 2016; Johansson et al., 2016).

188 **2.3.6 Vaccination**

189 We examined the effects of a potential ZIKV vaccine, given to 15-year-old-girls. This vaccination
190 strategy was used for rubella virus, which also causes congenital abnormalities, before the vaccine
191 was included in the measles, mumps and rubella vaccine given in childhood (Vyse et al., 2002). The
192 main objective of vaccination would be the prevention of adverse congenital outcomes, including
193 microcephaly. We simulated this intervention in the ABM, assuming vaccine implementation starting
194 in 2021, 2025 or 2031. From that date, half of the agents reaching age 15, representing females, could
195 transition to immune status R regardless of their initial status, with an effective vaccination coverage
196 ranging from 20% to 80%.

197 **2.4 Outcome analysis**

198 From the simulations, we collected 1) the evolution of the age-specific ZIKV immunity in the pop-
199 ulation; 2) the attack rate resulting from the reintroduction of ZIKV at year d ; 3) the age of newly
200 infected individuals. We fitted a binary Gaussian mixture model to dichotomize the observed attack
201 rates into either outbreaks or non-outbreaks. We defined the outbreak threshold as the 97.5% upper
202 bound of the lower distribution. This corresponded to a threshold of 1%, so that attack rates $\geq 1\%$
203 were considered as outbreaks. The age structure of newly infected individuals was used to compute
204 relative risks of infection by age group.

205 **3 Results**

206 **3.1 2016 ZIKV epidemic**

207 The fitted model (Figure 1), resulted in a reporting rate of 0.24% (95% credible interval, CrI: 0.21;
208 0.26). The transmission rate in the 0–14 age group was 42% (95% CrI: 35; 48) lower than in the
209 ≥ 15 age group. This corresponded to an overall basic reproduction number \mathcal{R}_0 of 1.58 (95% CrI:
210 1.56; 1.59). The predicted percentage of immune at the end of the epidemic was 36% (95% CrI: 34;
211 38) for the 0–14 age group and 53% (95% CrI: 50; 57) for the ≥ 15 age group.

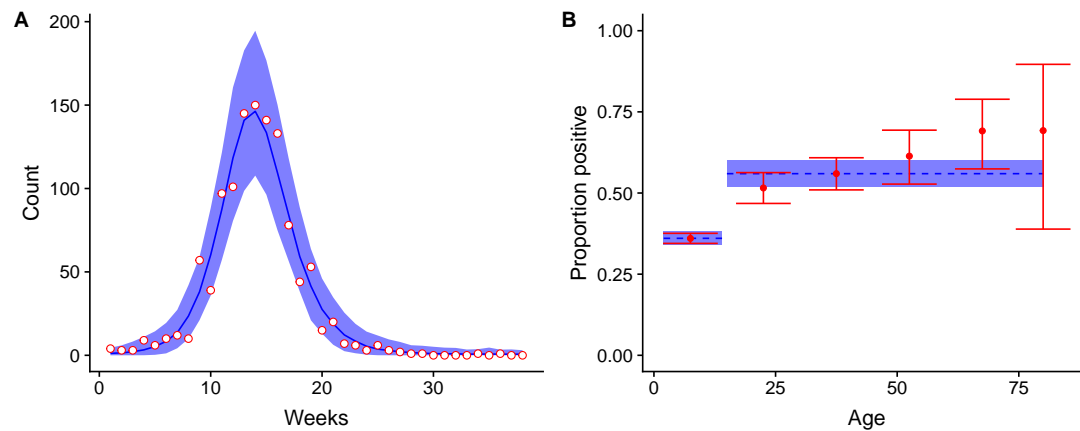


Figure 1: Model fit for (A) weekly incidence data and (B) post-epidemic sero-prevalence data from the 2016 ZIKV epidemic in Managua, Nicaragua. Data points are in red and the corresponding model fit (posterior median and 95% credible interval) is in blue.

212 3.2 Immunity and population

213 In our forward simulations, the expected population size increased by 42% between 2017 and 2097.
214 Under the assumption that ZIKV infection results in lifelong protective immunity, population re-
215 newal will create an imbalance in the proportion immune in different age groups. We expect the
216 overall proportion of the population with protective immunity to have halved (from 48% to 24%)
217 by 2051 and to be concentrated among the older age classes (Fig. 2A). The 0–14 year old age group
218 will become entirely susceptible by 2031 and the 15–29 year old age group by 2046.

219 3.3 Future risk of ZIKV outbreak

220 Reintroductions of ZIKV in the population of Managua are unlikely to develop into sizeable outbreaks
221 before 2035, 24 years after the 2016 epidemic, assuming lifelong immunity for individuals infected in
222 2016 (Fig. 2B). After this point, attack rates resulting from ZIKV reintroduction will rise steeply.
223 By 2047, we predict that ZIKV reintroductions will have a 50% probability of resulting in outbreaks
224 with attack rates greater than 1% (Fig. 2C).

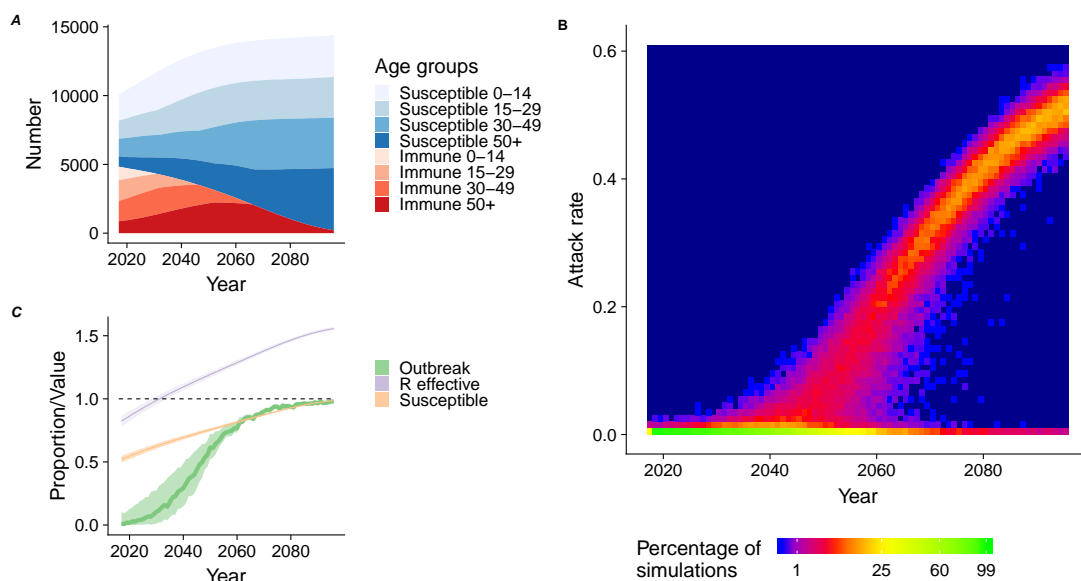


Figure 2: (A) The evolution of the immunity status per age group in a population of 10,000 agents for the next 80 years based on the demographic structure of Nicaragua. (B) Heat map of the distribution of the attack rates resulting from the reintroduction of ZIKV in the population at each year (1000 simulations for each year). (C) The evolution of the proportion of reintroductions resulting in outbreaks (with a threshold of 1%) with time (green), proportion of susceptible (orange), and effective reproduction number \mathcal{R}_e (purple).

225 3.4 Risk of infection and microcephaly births in women of reproductive 226 age

227 The differences between age groups in both immunity and transmission will result in a disproportional
228 burden of infection in the 15–29 age class. The relative risk of infection in this age group
229 ranges from 1.2 to 1.6, compared with the general population if an outbreak occurs during the period
230 2032–2075 (Fig. 3A). As most pregnancies occur in this age group, these women are also the
231 most likely to experience a pregnancy with an adverse outcome. The increased risk of infection in
232 this group implies that the number of adverse congenital outcomes resulting from a ZIKV outbreak
233 during this period is likely to be higher than expected with a homogeneous distribution of immunity
234 across ages. Assuming different values for the added risk of microcephaly after a ZIKV infection
235 during the first trimester, we expect the mean number of additional microcephaly cases due to ZIKV
236 infection resulting from the reintroduction of the virus in Managua, Nicaragua to reach 1 to 5 cases
237 per 100,000 population in 2060 (Fig. 3B).

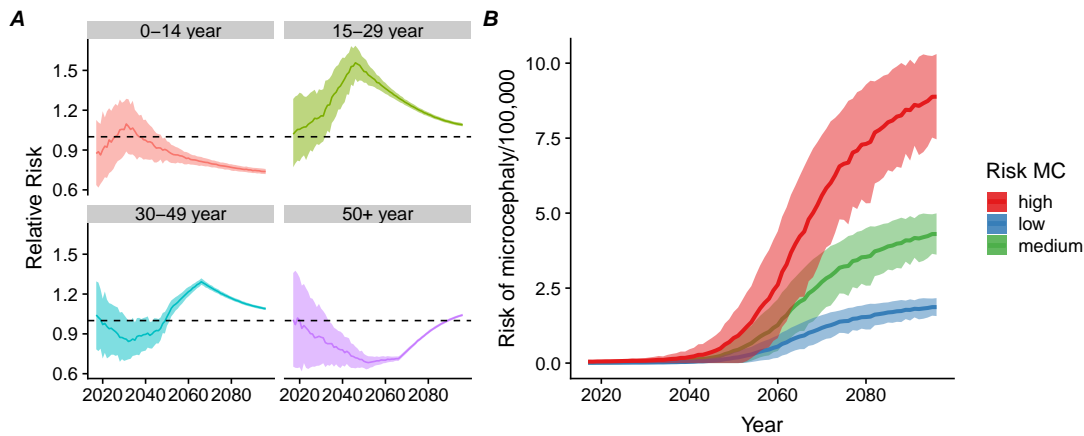


Figure 3: (A) Relative risk of ZIKV infection during a ZIKV outbreak per age group compared to the general population by year (median, interquartile range). (B) Expected number of additional microcephaly events associated with ZIKV infection during pregnancy per 100,000 total population according to three different risk scenarios.

238 3.5 Loss of immunity

239 If protective immunity to ZIKV is not lifelong, the time window before observing a rise in the attack
240 rates resulting from ZIKV reintroduction will shorten (Fig. 4A). For instance, if 15% of the those
241 who were infected in 2016 lose their immunity after 10 years (a mean duration of immunity of 60
242 years), the time until the risk of outbreak upon reintroduction reaches 50% would be 14 years earlier
243 (2033) than with lifelong immunity (2047). Loss of immunity over time would reduce the relative
244 risk in the 15–29 year old age group (Fig. 4B).

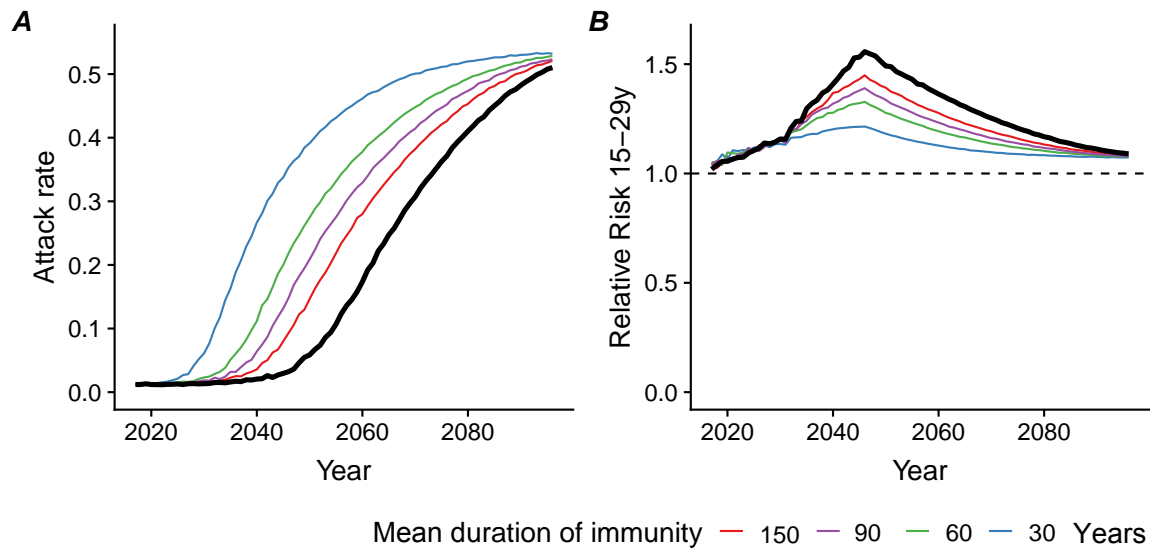


Figure 4: Consequences of alternative scenarios regarding the mean duration of protective immunity (30, 60 and 150 years), compared with lifelong immunity (thick black line): (A) median attack rate of ZIKV among reintroductions resulting in outbreaks (with a threshold of 1%) and (B) relative risk of ZIKV infection during an outbreak in the 15–29 year age group compared with the general population.

245 3.6 Targeted vaccination

246 The implementation of a vaccination program targeted towards 15 year old girls between 2021 and
247 2031 would reduce the risk of infection in women aged 15-29 years and would also indirectly reduce
248 the overall risk of a ZIKV outbreak in the population (Fig. 5). If effective vaccine coverage is
249 60–80% amongst 15 year old girls, the prolongation of herd immunity could effectively mitigate the
250 overall risk of a ZIKV outbreak in the population. The reduction in the number of microcephaly
251 cases would then exceed what would be expected by considering only the direct protection granted
252 by a vaccine to future mothers. A later implementation of the intervention would be less effective,
253 as it becomes more difficult to maintain the herd immunity (Fig. 5B).

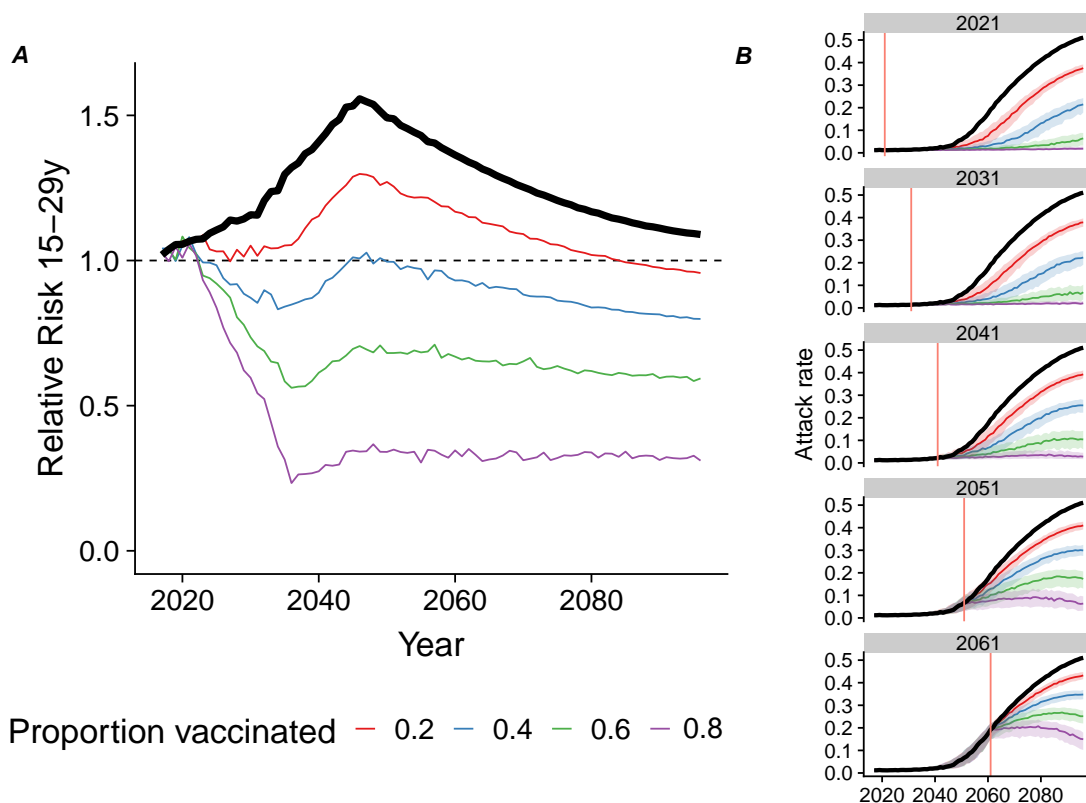


Figure 5: Consequences of implementing a targeted vaccination program among 15-year-old-girls from 2021 onwards with various levels of effective vaccination coverage (from 20 to 80%) compared with no vaccination (thick black line): (A) relative risk of ZIKV infection during an outbreak in the 15–29 year age group compared with the general population and (B) attack rate of ZIKV among reintroductions resulting in outbreaks (median, interquartile range, with a threshold of 1%), when vaccination is introduced from 2021, 2031, 2041, 2051 or 2061 onwards (red vertical line).

254 4 Discussion

255 In this mathematical modelling study, we show that a new ZIKV outbreak in Nicaragua would affect
 256 proportionally more women in the young reproductive age range (15–29 years) than the general
 257 population, owing to the age-dependent infection pattern and population renewal. The risk of a
 258 new ZIKV outbreak in Nicaragua, after reintroduction, will remain low before 2035 because of herd
 259 immunity, then rise to 50% in 2047. If protective immunity to ZIKV decays with time, ZIKV
 260 recurrence could occur sooner. Timely introduction of targeted vaccination, focusing on females
 261 aged 15 years would both reduce the risk of adverse congenital outcomes and extend herd immunity,
 262 mitigating the overall risk of an outbreak and resulting in lower attack rates if an outbreak occurs.

263 4.1 Strengths and limitations of the study

264 A strength of our approach is that it allows for the full propagation of uncertainty from the initial
 265 data into the risk assessment, by transferring the posterior distributions of the parameters from
 266 the deterministic model fitted to surveillance and seroprevalence data on the 2016 epidemic into

267 the ABM used for simulations. Roche et al. showed that, when a sufficiently small time step was
268 chosen, stochastic and deterministic models using the same parameter values led to similar results
269 (Roche et al., 2011b). Additionally, we benefited from the availability of high quality data from
270 population-based surveys that included participants from age 2 to 80 years in Managua, Nicaragua.
271 The age-stratified seroprevalence data allowed us to investigate the risk in different age groups and
272 better assess the evolution of the age-specific immunity, which is crucial when studying adverse
273 congenital events caused by ZIKV infection during pregnancy.

274 We chose a simple approach based on an SIR structure, similar to the model used by Netto et al.,
275 to focus on the dynamics of infection and immunity in the human population. We did not model
276 vector populations and behavior explicitly, as in some other studies (Kucharski et al., 2016; Cham-
277 pagne et al., 2016; Ferguson et al., 2016). This simplification limits the mechanistic interpretation of
278 the epidemic parameters, but provides a phenomenological description of the transmission dynamics.
279 We believe that this approach is appropriate because our main objective was to determine the risk
280 of an outbreak after reintroduction of ZIKV, which is mostly influenced by the level of protective
281 immunity in the human population. We acknowledge that the future occurrence of ZIKV in the area
282 also depends on the presence of a competent vector. Our choice is supported by sensitivity analyses
283 that show that more complex model structures (delayed SIR and Ross-MacDonald-type models)
284 were not superior to a simple SIR structure in describing the 2016 ZIKV epidemic of Managua
285 (Appendix A.6). Similarly, Pandey et al. (2013) showed that additional model complexity does not
286 result in a better description of the dynamics of transmission of dengue virus (another Aedes-borne
287 virus) in a human population compared with a SIR model (Pandey et al., 2013). In our model,
288 the transmission rate (β_a) captures both human-mosquito and mosquito-human transmission; we
289 assumed a constant transmission rate, as observed in the 2016 outbreak.

290 Another limitation of our model is that we did not take migration or changes in population
291 distribution into account in our model. An influx of people with lower levels of protective immunity
292 or higher birth rates would increase the speed at which the population becomes susceptible again.
293 Nicaragua has an urbanization rate that exceeds the world average (Maria et al., 2017). If rural
294 populations have lower seroprevalence for ZIKV, as was shown in Suriname (Langerak et al., 2019),
295 an inflow of rural inhabitants into Managua could increase the risk of ZIKV outbreaks. Uncertainty
296 remains, as factors such as the political instability in Nicaragua could drive migration and influence
297 disease transmission, as we currently observe in Venezuela and bordering countries (Tuite et al.,
298 2018).

299 4.2 Interpretation in comparison with other studies

300 This study shows that the lower attack rate of ZIKV in children than in adults will hasten the
301 emergence of a population that will be fully susceptible to infection, especially if immunity is not
302 lifelong. The advantage of our approach is that we used the age-specific attack rates to model
303 the processes of ageing in relation to protective immunity to ZIKV explicitly. Even with lifelong
304 immunity, our model predicts that children aged 0–14 years will become entirely susceptible by 2031
305 and 15–29 year olds by 2046. In future outbreaks, the attack rate will then be highest amongst
306 15–29 year olds, including women who will be at risk of ZIKV infection in pregnancy. If immunity
307 wanes, the time until the next ZIKV outbreak will be reduced and, in that case, the distribution of
308 infection risk would be more equal across age groups (Fig. 4). Several authors have studied the time
309 to a next ZIKV outbreak, but none studied the effect of the loss of immunity over time in relation to
310 age. Assuming lifelong immunity, our estimates of the time until the risk increases are similar to the
311 12–20 years before re-emergence estimated for French Polynesia (Kucharski et al., 2016). Netto et al
312 (2017) used an SEIR model to show that in Salvador, Brazil, the effective reproduction number was
313 insufficient to cause a new outbreak during the “subsequent years” (Netto et al., 2017). Lourenço
314 (2017) showed the same for the whole of Brazil: herd immunity should protect the population from
315 a new outbreak in the coming years (Lourenço et al., 2017). Ferguson et al. (2016) concluded that

316 the age distribution of future ZIKV outbreaks will likely differ and that a new large epidemic will
317 be delayed for “at least a decade” (Ferguson et al., 2016).

318 Other ZIKV vaccination studies confirm our findings. However, they do not show the effect in
319 risk groups nor assume herd immunity from previous outbreaks like we did here; Durham et al.
320 (2018) showed that immunizing females aged 9 to 49 years with a 75% effective vaccine and a
321 coverage of 90%, would reduce the incidence of prenatal infections by at least 94%. Similarly,
322 Bartsch et al. (2018) showed that women of childbearing age or young adults would be an ideal
323 target group for vaccination. Valega-Mackenzie and Ríos-Soto (2018) formulated a vaccination model
324 for ZIKV transmission that included mosquito and sexual transmission. They found that vaccination
325 works if well administered, both when sexual transmission is most important and when vector-born
326 transmission is most important.

327 **4.3 Implications and future research**

328 Our finding that people in the 15–29 age range are more at risk of infection implies that we expect
329 a higher number of congenital abnormalities due to ZIKV infection. Thus, vaccine development
330 efforts should be increased. Our conclusions are drawn based on data from Managua, Nicaragua,
331 but should be relevant to many regions in the Americas and the Pacific that have documented high
332 post-epidemic levels of seropositivity (Aubry et al., 2017; Netto et al., 2017; Saba Villarroel et al.,
333 2018). In regions where ZIKV has not yet caused an epidemic but competent vectors are present,
334 vaccination would be in place as well. Further age-stratified seroprevalence studies, using sensitive
335 and specific tests and with longitudinal follow-up, are needed to improve our understanding of ZIKV
336 antibody distribution in populations and to quantify the duration of immunity. This information
337 will provide important information to improve mathematical modeling of ZIKV risk.

338 ZIKV vaccine development faces considerable hurdles. First, the evaluation of vaccine efficacy
339 has stalled because the reduced circulation of ZIKV has reduced the visibility of ZIKV-associated
340 disease (Cohen, 2018). Second, it remains unclear if neutralizing antibodies induced by vaccination
341 are sufficient to protect women against vertical transmission and congenital abnormalities (Diamond
342 et al., 2018). Third, it is not clear whether or how vaccine-induced antibodies against ZIKV will
343 cross-react with other flaviviruses. To move vaccine development forward, we need to find regions
344 where disease will occur to be able to conduct trials. This requires identifying populations that are
345 at risk, and implementing surveillance there. These can either be regions where ZIKV is endemic, or
346 where ZIKV outbreaks are likely to occur; throughout the Americas, there might be regions that did
347 not experience an outbreak, but do have suitable conditions such as competent vectors. Conducting
348 vaccine trials in disease outbreaks is complex, but there are tools to facilitate planning (Bellan et al.,
349 2019). ZIKV in an endemic setting, such as in Africa and Asia, could prove a suitable setting as
350 well. However, ZIKV circulation in endemic setting is not well described and the occurrence of
351 adverse outcomes in this context is less documented Counotte et al. (2018). Further research in
352 understanding the transmission of the virus in an endemic context is therefore needed.

353 **4.4 Conclusion**

354 Preparedness is vital; the time until the next outbreak gives us to opportunity to be prepared.
355 The next sizeable ZIKV outbreak in Nicaragua will likely not occur before 2035 but the probability
356 of outbreaks will increase. Young women of reproductive age will be at highest risk of infection
357 during the next ZIKV outbreak. Vaccination targeted to young women could curb the risk of a
358 large outbreak and extend herd immunity. ZIKV vaccine development and licensure are urgent to
359 attain the maximum benefit in reducing the population-level risk of infection and the risk of adverse
360 congenital outcomes. The urgency of ZIKV vaccine development increases if immunity is not lifelong.

361 5 Acknowledgments

362 Calculations were performed on UBELIX (<http://www.id.unibe.ch/hpc>), the HPC cluster at the
363 University of Bern. MJC received salary support from the Swiss National Science Foundation
364 (project grant 320030_176233).

365 6 Competing interests

366 References

367 **Abbink P**, Stephenson KE, Barouch DH. Zika virus vaccines. *Nat Rev Microbiol.* 2018; 16(10):594–
368 600. doi: 10.1038/s41579-018-0039-7.

369 **Aubry M**, Teissier A, Huart M, Merceron S, Vanhomwegen J, Roche C, Vial AL, Teururai S,
370 Sicard S, Paulous S, Desprès P, Manuguerra JC, Mallet HP, Musso D, Deparis X, Cao-Lormeau
371 VM. Ross river virus seroprevalence, French Polynesia, 2014–2015. *Emerg Infect Dis.* 2017;
372 23(10):1751–1753. doi: 10.3201/eid2310.170583.

373 **Balmaseda A**, Stettler K, Medialdea-Carrera R, Collado D, Jin X, Zambrana JV, Jaconi S,
374 Camerini E, Saborio S, Rovida F, Percivalle E, Ijaz S, Dicks S, Ushiro-Lumb I, Barzon L, Siqueira
375 P, Brown DWG, Baldanti F, Tedder R, Zambon M, et al. Antibody-based assay discriminates
376 Zika virus infection from other flaviviruses. *Proc Natl Acad Sci.* 2017; 114(31):8384–8389. doi:
377 10.1073/pnas.1704984114.

378 **Bartsch SM**, Asti L, Cox SN, Durham DP, Randall S, Hotez PJ, Galvani AP, Lee BY. What Is
379 the Value of Different Zika Vaccination Strategies to Prevent and Mitigate Zika Outbreaks? *J*
380 *Infect Dis.* 2018 dec; <https://doi.org/10.1093/infdis/jiy688>, doi: 10.1093/infdis/jiy688.

381 **Bellan SE**, Eggo RM, Gsell PS, Kucharski AJ, Dean NE, Donohue R, Zook M, Edmunds
382 WJ, Odhiambo F, Longini IM, Brisson M, Mahon BE, Henao-Restrepo AM. An online de-
383 cision tree for vaccine efficacy trial design during infectious disease epidemics: The InterVax-
384 Tool. *Vaccine.* 2019; 37(31):4376–4381. [http://www.sciencedirect.com/science/article/
385 pii/S0264410X19307807](http://www.sciencedirect.com/science/article/pii/S0264410X19307807), doi: 10.1016/j.vaccine.2019.06.019.

386 **Cao-Lormeau VM**, Roche C, Teissier A, Robin E, Berry AL, Mallet HP, Sall AA, Musso D.
387 Zika Virus, French Polynesia, South Pacific, 2013. *Emerg Infect Dis.* 2014; 20(6):1085. doi:
388 10.3201/eid2006.140138.

389 **Carpenter B**, Gelman A, Hoffman MD, Lee D, Goodrich B, Betancourt M, Brubaker M, Guo J,
390 Li P, Riddell A. Stan : A Probabilistic Programming Language. *J Stat Softw.* 2017; 76(1). doi:
391 10.18637/jss.v076.i01.

392 **Cauchemez S**, Besnard M, Bompard P, Dub T, Guillemette-Artur P, Eyrolle-Guignot D, Salje H,
393 Van Kerkhove MD, Abadie V, Garel C, Fontanet A, Mallet HP. Association between Zika virus and
394 microcephaly in French Polynesia, 2013–15: A retrospective study. *Lancet.* 2016; 387(10033):2125–
395 2132. doi: 10.1016/S0140-6736(16)00651-6.

396 **Champagne C**, Salthouse DG, Paul R, Cao-Lormeau VM, Roche B, Cazelles B. Structure in the
397 variability of the basic reproductive number (R_0) for Zika epidemics in the Pacific islands. *Elife.*
398 2016 nov; 5(NOVEMBER2016). doi: 10.7554/eLife.19874.

399 **Cohen J**. Steep drop in Zika cases undermines vaccine trial. *Science.* 2018; 361(6407):1055–1056.
400 doi: 10.1126/science.361.6407.1055.

- 401 **Counotte MJ**, Egli-Gany D, Riesen M, Abraha M, Porgo TV, Wang J, Low N. Zika
402 virus infection as a cause of congenital brain abnormalities and Guillain-Barré syndrome:
403 From systematic review to living systematic review. *F1000Research*. 2018; 7(196):196. doi:
404 10.12688/f1000research.13704.1.
- 405 **Diamond MS**, Ledgerwood JE, Pierson TC. Zika Virus Vaccine Development: Progress in the
406 Face of New Challenges. *Annu Rev Med*. 2018; 70(1):121–135. doi: 10.1146/annurev-med-040717-
407 051127.
- 408 **Diekmann O**, Heesterbeek JAP, Roberts MG. The construction of next-generation matri-
409 ces for compartmental epidemic models. *J R Soc Interface*. 2010; 7(47):873–885. doi:
410 10.1098/rsif.2009.0386.
- 411 **Dietz K**. Transmission and control of arbovirus diseases. *Epidemiology*. 1975; 104:104–121.
- 412 **Duffy MR**, Chen TH, Hancock WT, Powers AM, Kool JL, Lanciotti RS, Pretrick M, Marfel M,
413 Holzbauer S, Dubray C, Guillaumot L, Griggs A, Bel M, Lambert AJ, Laven J, Kosoy O, Panella
414 A, Biggerstaff BJ, Fischer M, Hayes EB. Zika Virus Outbreak on Yap Island, Federated States of
415 Micronesia. *N Engl J Med*. 2009; 360(24):2536–2543. doi: 10.1056/NEJMoa0805715.
- 416 **Durham DP**, Fitzpatrick MC, Ndeffo-Mbah ML, Parpia AS, Michael NL, Galvani AP. Evaluating
417 vaccination strategies for zika virus in the Americas. *Ann Intern Med*. 2018 may; 168(9):621–630.
418 <https://doi.org/10.7326/M17-0641>, doi: 10.7326/M17-0641.
- 419 **Faria NR**, Do Socorro Da Silva Azevedo R, Kraemer MUG, Souza R, Cunha MS, Hill SC, Thézé
420 J, Bonsall MB, Bowden TA, Rissanen I, Rocco IM, Nogueira JS, Maeda AY, Da Silva Vasami
421 FG, De Lima Macedo FL, Suzuki A, Rodrigues SG, Cruz ACR, Nunes BT, De Almeida Medeiros
422 DB, et al. Zika virus in the Americas: Early epidemiological and genetic findings. *Science*. 2016;
423 352(6283):345–349. doi: 10.1126/science.aaf5036.
- 424 **Ferguson NM**, Cucunubá ZM, Dorigatti I, Nedjati-Gilani GL, Donnelly CA, Basáñez MG, Nouvel-
425 let P, Lessler J. Countering the Zika epidemic in Latin America. *Science*. 2016; 353(6297):353–354.
426 doi: 10.1126/science.aag0219.
- 427 **Gaudinski MR**, Houser KV, Morabito KM, Hu Z, Yamshchikov G, Rothwell RS, Berkowitz N,
428 Mendoza F, Saunders JG, Novik L, Hendel CS, Holman LSA, Gordon IJ, Cox JH, Edupuganti S,
429 McArthur MA, Roupheal NG, Lyke KE, Cummings GE, Sitar S, et al. Safety, tolerability, and im-
430 munogenicity of two Zika virus DNA vaccine candidates in healthy adults: randomised, open-label,
431 phase 1 clinical trials. *Lancet*. 2018; 391(10120):552–562. doi: 10.1016/S0140-6736(17)33105-7.
- 432 **Guan Y**. Variance stabilizing transformations of Poisson, binomial and negative binomial distribu-
433 tions. *Stat Probab Lett*. 2009; 79(14):1621–1629. doi: 10.1016/j.spl.2009.04.010.
- 434 **Haby MM**, Pinart M, Elias V, Reveiz L. Prevalence of asymptomatic Zika virus infection: A
435 systematic review. *Bull World Health Organ*. 2018; 96(6):402–413D. doi: 10.2471/BLT.17.201541.
- 436 **Henderson AD**, Aubry M, Kama M, Vanhomwegen J, Teissier A, Mariteragi-Helle T, Paoaafaite T,
437 Manuguerra JC, Edmunds WJ, Whitworth J, Watson CH, Lau CL, Cao-Lormeau VM, Kucharski
438 AJ. Zika virus seroprevalence declines and neutralization antibodies wane in adults following
439 outbreaks in French Polynesia and Fiji. *bioRxiv*. 2019; p. 578211. [http://biorxiv.org/content/
440 early/2019/03/15/578211.abstract](http://biorxiv.org/content/early/2019/03/15/578211.abstract), doi: 10.1101/578211.
- 441 **Johansson MA**, Mier-Y-Teran-Romero L, Reefhuis J, Gilboa SM, Hills SL. Zika and the risk of
442 Microcephaly. *Obstet Gynecol Surv*. 2016; 71(11):635–636. doi: 10.1097/OGX.0000000000000386.

- 443 **Kohl A**, Gatherer D. Zika virus: a previously slow pandemic spreads rapidly through the Americas.
444 *J Gen Virol.* 2015; 97(2):269–273. doi: 10.1099/jgv.0.000381.
- 445 **Krauer F**, Riesen M, Reveiz L, Oladapo OT, Martínez-Vega R, Porgo TV, Haefliger A, Broutet NJ,
446 Low N. Zika Virus Infection as a Cause of Congenital Brain Abnormalities and Guillain–Barré Syn-
447 drome: Systematic Review. *PLoS Med.* 2017; 14(1):e1002203. doi: 10.1371/journal.pmed.1002203.
- 448 **Kucharski AJ**, Funk S, Eggo RM, Mallet HP, Edmunds WJ, Nilles EJ. Transmission Dynamics of
449 Zika Virus in Island Populations: A Modelling Analysis of the 2013–14 French Polynesia Outbreak.
450 *PLoS Negl Trop Dis.* 2016; 10(5):e0004726. doi: 10.1371/journal.pntd.0004726.
- 451 **Langerak T**, Brinkman T, Mumtaz N, Arron G, Hermelijn S, Baldewsingh G, Wongsokarijo M,
452 Resida L, Rockx B, Koopmans MPG, Van Gorp ECM, Vreden S. Zika Virus Seroprevalence in
453 Urban and Rural Areas of Suriname, 2017. *J Infect Dis.* 2019; doi: 10.1093/infdis/jiz063.
- 454 **Lourenço J**, de Lima MM, Faria NR, Walker A, Kraemer MUG, Villabona-Arenas CJ, Lambert B,
455 de Cerqueira EM, Pybus OG, Alcantara LCJ, Recker M. Epidemiological and ecological determi-
456 nants of Zika virus transmission in an urban setting. *Elife.* 2017 sep; 6. doi: 10.7554/eLife.29820.
- 457 **Maria A**, Acero JL, Aguilera AI, Lozano MG. Central America Urbanization Review: Making
458 Cities Work for Central America. The World Bank; 2017. doi: 10.1596/978-1-4648-0985-9.
- 459 **Modjarrad K**, Lin L, George SL, Stephenson KE, Eckels KH, De La Barrera RA, Jarman RG,
460 Sondergaard E, Tennant J, Ansel JL, Mills K, Koren M, Robb ML, Barrett J, Thompson J, Kosel
461 AE, Dawson P, Hale A, Tan CS, Walsh SR, et al. Preliminary aggregate safety and immuno-
462 genicity results from three trials of a purified inactivated Zika virus vaccine candidate: phase 1,
463 randomised, double-blind, placebo-controlled clinical trials. *Lancet.* 2018; 391(10120):563–571.
464 doi: 10.1016/S0140-6736(17)33106-9.
- 465 **National Institute of Allergy and Infectious Diseases**, VRC 705: A Zika Virus DNA
466 Vaccine in Healthy Adults and Adolescents (DNA); 2018. [Online]. Available from: <https://clinicaltrials.gov/ct2/show/NCT03110770>.
467
- 468 **Netto EM**, Moreira-Soto A, Pedroso C, Höser C, Funk S, Kucharski AJ, Rockstroh A, Küm-
469 merer BM, Sampaio GS, Luz E, Vaz SN, Dias JP, Bastos FA, Cabral R, Kistemann T, Ulbert
470 S, de Lamballerie X, Jaenisch T, Brady OJ, Drosten C, et al. High Zika Virus Seroprevalence in
471 Salvador, Northeastern Brazil Limits the Potential for Further Outbreaks. *MBio.* 2017; 8(6). doi:
472 10.1128/mbio.01390-17.
- 473 **PAHO**, PAHO - Cumulative Incidence; 2019. [Online]. Available from: https://www.paho.org/hq/index.php?option=com_content&view=article&id=12390:zika-cumulative-cases&Itemid=42090&lang=en.
474
475
- 476 **Pandey A**, Mubayi A, Medlock J. Comparing vector-host and SIR models for dengue transmission.
477 *Math Biosci.* 2013; 246(2):252–259. doi: 10.1016/j.mbs.2013.10.007.
- 478 **R Core Team**, Team RDC. R: A Language and Environment for Statistical Computing. Vienna,
479 Austria; 2008.
- 480 **Roche B**, Drake JM, Rohani P. An Agent-Based Model to study the epidemiological and evolu-
481 tionary dynamics of Influenza viruses. *BMC Bioinformatics.* 2011; 12(1):87. doi: 10.1186/1471-
482 2105-12-87.
- 483 **Roche B**, Drake JM, Rohani P. An Agent-Based Model to study the epidemiological and evolu-
484 tionary dynamics of Influenza viruses. *BMC Bioinformatics.* 2011; 12(1). doi: 10.1186/1471-2105-
485 12-87.

- 486 **Saba Villarroel PM**, Nurtop E, Pastorino B, Roca Y, Drexler JF, Gallian P, Jaenisch T, Leparco-
487 Goffart I, Priet S, Ninove L, de Lamballerie X. Zika virus epidemiology in Bolivia: A sero-
488 prevalence study in volunteer blood donors. *PLoS Negl Trop Dis*. 2018; 12(3):e0006239. doi:
489 10.1371/journal.pntd.0006239.
- 490 **Tuite AR**, Thomas-Bachli A, Acosta H, Bhatia D, Huber C, Petrasek K, Watts A, Yong JHE, Bo-
491 goch II, Khan K. Infectious disease implications of large-scale migration of Venezuelan nationals.
492 *J Travel Med*. 2018 sep; 25(1). doi: 10.1093/jtm/tay077.
- 493 **Valega-Mackenzie W**, Ríos-Soto KR. Can Vaccination Save a Zika Virus Epidemic? *Bull Math*
494 *Biol*. 2018 mar; 80(3):598–625. doi: 10.1007/s11538-018-0393-7.
- 495 **Vyse AJ**, Gay NJ, White JM, Ramsay ME, Brown DWG, Cohen BJ, Hesketh LM, Morgan-Capner
496 P, Miller E. Evolution of surveillance of measles, mumps, and rubella in England and Wales:
497 Providing the platform for evidence-based vaccination policy. *Epidemiol Rev*. 2002; 24(2):125–
498 136. doi: 10.1093/epirev/mxf002.
- 499 **Wikan N**, Smith DR. Zika virus: History of a newly emerging arbovirus. *Lancet Infect Dis*. 2016;
500 16(7):e119–e126. doi: 10.1016/S1473-3099(16)30010-X.
- 501 **World Bank**, World Development Indicators; 2019. [Online]. Available from: [https://data.](https://data.worldbank.org/indicator/SP.DYN.TFRT.IN?locations=NI)
502 [worldbank.org/indicator/SP.DYN.TFRT.IN?locations=NI](https://data.worldbank.org/indicator/SP.DYN.TFRT.IN?locations=NI).
- 503 **World Bank**, World Development Indicators; 2019. [Online]. Available from: [https://databank.](https://databank.worldbank.org/data/reports.aspx?source=2&series=SP.POP.TOTL.MA.IN&country=NIC)
504 [worldbank.org/data/reports.aspx?source=2&series=SP.POP.TOTL.MA.IN&country=NIC](https://databank.worldbank.org/data/reports.aspx?source=2&series=SP.POP.TOTL.MA.IN&country=NIC).
- 505 **World Health Organization**. WHO statement on the first meeting of the International Health
506 Regulations (2005) (IHR 2005) Emergency Committee on Zika virus and observed increase in
507 neurological disorders and neonatal malformations. WHO. 2016; .
- 508 **World Health Organization**, WHO Malaria Vaccine Pipeline Tracker; 2018. [Online].
509 Available from: [https://www.who.int/immunization/research/vaccine_pipeline_tracker_](https://www.who.int/immunization/research/vaccine_pipeline_tracker_spreadsheet/en/)
510 [spreadsheet/en/](https://www.who.int/immunization/research/vaccine_pipeline_tracker_spreadsheet/en/).
- 511 **World Health Organization**, WHO | By Category | Life Tables by Country - Nicaragua. World
512 Health Organization; 2019. [Online]. Available from: [http://apps.who.int/gho/data/?theme=](http://apps.who.int/gho/data/?theme=main&vid=61180)
513 [main&vid=61180](http://apps.who.int/gho/data/?theme=main&vid=61180).
- 514 **Zambrana JV**, Bustos Carrillo F, Burger-Calderon R, Collado D, Sanchez N, Ojeda S, Carey Mon-
515 terrey J, Plazaola M, Lopez B, Arguello S, Elizondo D, Aviles W, Coloma J, Kuan G, Balmaseda
516 A, Gordon A, Harris E. Seroprevalence, risk factor, and spatial analyses of Zika virus infection
517 after the 2016 epidemic in Managua, Nicaragua. *Proc Natl Acad Sci*. 2018; 115(37):9294–9299.
518 doi: 10.1073/pnas.1804672115.
- 519 **Zhang Q**, Sun K, Chinazzi M, Pastore Y Piontti A, Dean NE, Rojas DP, Merler S, Mistry D,
520 Poletti P, Rossi L, Bray M, Halloran ME, Longini IM, Vespignani A. Spread of Zika virus in the
521 Americas. *Proc Natl Acad Sci U S A*. 2017; 114(22):E4334–E4343. doi: 10.1073/pnas.1620161114.

522 Appendices

523 A Appendix

524 A.1 ABM algorithm

525 Here, we provide the pseudo code of the ABM (Algorithm 1).

Algorithm 1 ABM

```
1: procedure INITIALIZATION ▷ Add initial conditions S/R and sex per  $n$  individual
2:   for  $n \leftarrow 1, popMax$  do
3:      $R[n] \leftarrow$  select random 1 or 0 with probability(age[n])
4:      $S[n] \leftarrow 1 - R[n]$ 
5:      $I[n] \leftarrow 0$ 
6:     sex[n]  $\leftarrow$  select random 1 or 0 with probability 0.5
7:   end for
8: end procedure
9: procedure SIMULATION ▷ Simulation over  $wkMax$  weeks
10:  for  $wk \leftarrow 1, wkMax$  do
11:    for  $n \leftarrow 1, popMax$  do ▷ Loop over  $popMax$  individuals
12:      if individual is alive then
13:        procedure POPULATION DYNAMICS ▷ Pre-outbreak
14:          Birth, Death, Ageing
15:        end procedure
16:        procedure LOSS OF IMMUNITY ▷ Loss of immunity
17:           $[R \rightarrow S]$  with probability RateToProb( $\xi$ )
18:        end procedure
19:        procedure VACCINATION ▷ Vaccination
20:           $[S \rightarrow R]$  with probability vaccinationProb, at  $age[n]$ 
21:        end procedure
22:        procedure INFECTION, RECOVERY ▷ During outbreak
23:           $[S \rightarrow I]$  with probability RateToProb( $\beta, age[n]$ )
24:           $[I \rightarrow R]$  with probability RateToProb( $\gamma$ )
25:        end procedure
26:      end if
27:    end for
28:    procedure START OUTBREAK ▷ Introduction of infection
29:      if  $wk = introductionWk$  then
30:        Change timestep: 7 days to 0.1 days
31:        Collect summary statistics pre-outbreak
32:        Introduce  $introductionN$  infections
33:      end if
34:    end procedure
35:    total number alive ▷ Collect summary of week  $wk$ :
36:    total number infected
37:  end for
38: end procedure
```

526 A.2 \mathcal{R}_0

527 We used the next generation matrix method described by Diekmann et al. to calculate \mathcal{R}_0 (eq. 8
528 - 10). β_1 is the transmission rate for the 0–14 age group; β_2 for the >15 group; γ is the common
529 recovery rate.

$$F = \begin{pmatrix} \beta_1 & \beta_1 \\ \beta_2 & \beta_2 \end{pmatrix} \quad (8)$$

$$V = \begin{pmatrix} -\gamma & 0 \\ 0 & -\gamma \end{pmatrix} \quad (9)$$

$$\mathcal{R}_0 = \sqrt{\text{eig}(FV^{-1})} = \sqrt{\frac{\beta_1 + \beta_2}{\gamma}} \quad (10)$$

530 A.3 Loss of immunity scenarios

531 We explored plausible scenarios of loss of immunity (Fig. A.1).

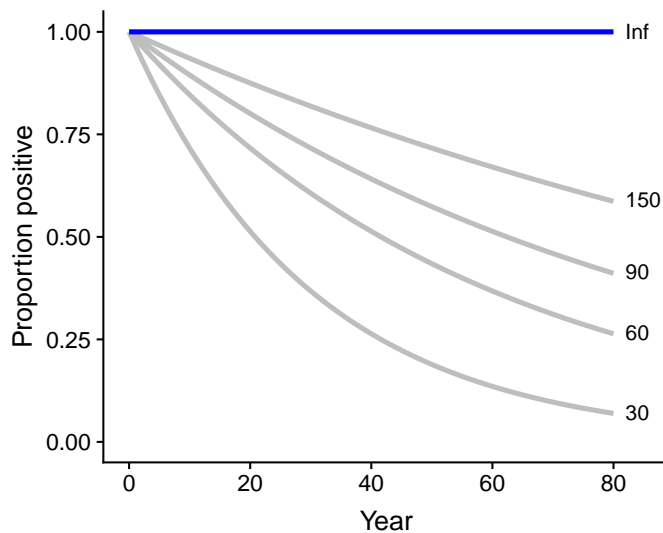


Figure A.1: Different scenarios of loss of immunity. No loss of immunity (blue) and scenarios explored (grey, exponential function with mean durations 30, 60, 90 and 150 years).

532 A.4 The number of infections introduced does influence the probability 533 of an outbreak, but not the attack rate of successful outbreaks

534 The proportion of outbreaks (1% threshold) after introduction depends on the number of infections
535 introduced; the attack rate of the successful outbreaks does not depend on the number of infections
536 introduced (Fig. A.2).

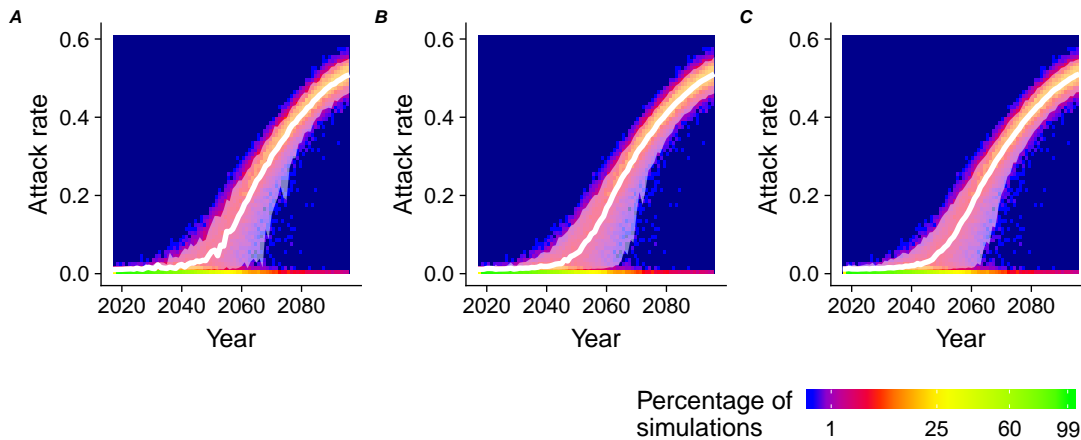


Figure A.2: Attack rate over time for the introduction of (A) $n=1$, (B) $n=5$, (C) $n=10$ infections.

537 **A.5 Once per simulation introduction vs once per year introduction of** 538 **infection**

539 Using the ABM (model B) we explored the effect of yearly introduction of one infectious individual
540 in the population ($n=10,000$). In the main text, we assumed a single introduction of n individuals
541 per simulation. Here we introduce on a yearly basis the infectious individuals; previous outbreaks
542 during the simulation affect the likelihood of a next outbreak and observed patterns are more
543 stochastic. However, the pattern of the attack rate over time remains similar to the findings of the
544 once/simulation introduction (Fig. A.3); the variation is larger due to a more stochasticity.

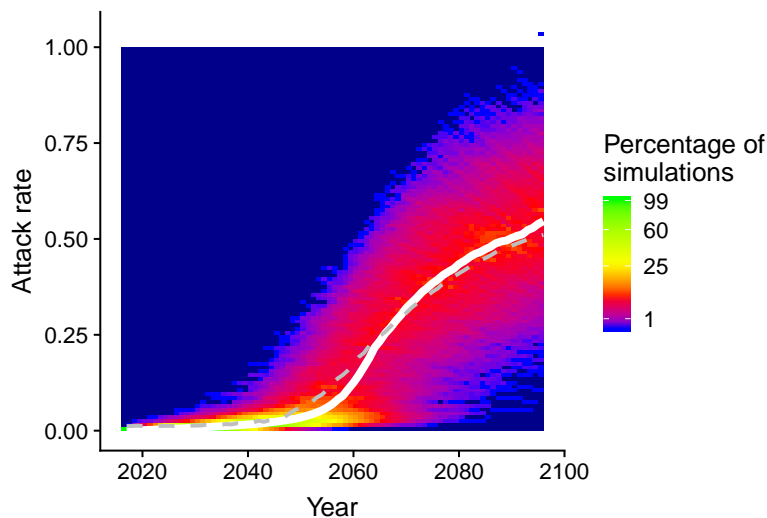


Figure A.3: Heat map of attack rate per time for simulations where every year one infectious individual is introduced in a population of 10,000. The median (white line) of this simulation is compared with the median of the simulation where once per simulation an infection is introduced (dashed grey line).

545 **A.6 Comparison of SIR model with SEIR model and the Pandey model.**

546 We compared the SIR model with a SEIR and model that explicitly models the vector; the Pandey
547 2013 model as implemented in Champagne et al. (2016) (Champagne et al., 2016). The model fit
548 of the more complex models does not outperform the fit of the simplest (SIR) model (Table A.1),
549 justifying the model choice.

Model	LOOIC (SE)	Δ LOOIC (SE)
SIR	95.2 (8.7)	Ref.
SEIR	93.9 (8.9)	-1.3 (1.6)
Pandey	99.5 (8.3)	4.3 (3.6)

Table A.1: Model comparison